



## Mobilisation of toxic trace elements under various beach nourishments<sup>☆</sup>



Iris R. Pit<sup>a,\*</sup>, Stefan C. Dekker<sup>a</sup>, Tobias J. Kanters<sup>a</sup>, Martin J. Wassen<sup>a</sup>, Jasper Griffioen<sup>a,b</sup>

<sup>a</sup> Copernicus Institute of Sustainable Development, Utrecht University, The Netherlands

<sup>b</sup> TNO Geological Survey, The Netherlands

### ARTICLE INFO

#### Article history:

Received 19 May 2017

Received in revised form

15 July 2017

Accepted 15 August 2017

#### Keywords:

Pyrite oxidation

Freshening

Coastal management

Trace elements

Decalcification

### ABSTRACT

To enhance protection and maintain wide beaches for recreation, beaches are replenished with sand: so-called beach nourishments. We compared four sites: two traditional beach nourishments, a mega beach nourishment and a reference without beach nourishment. Two sites contain calcareous-rich sand, whereas the other two sites have calcareous-poor sand. We aimed to understand hydrogeochemical processes to indicate factors critical for the mobility of trace elements at nourishments. We therefore analysed the chemical characteristics of sediment and pore water to ascertain the main drivers that mobilise toxic trace elements. With Dutch Quality Standards for soil and groundwater, the characteristics of sediment and pore water were compared to Target Values (the values at which there is a sustainable soil quality) and Intervention Values (the threshold above which the soil's functions are at risk). The pore water characteristics revealed that Target Values were regularly exceeded, especially for the nourishment sites and mainly for Mo (78%), Ni (24%), Cr (55%), and As (21%); Intervention Values for shallow groundwater were occasionally exceeded for As (2%), Cr (2%) and Zn (2%). The sediment characteristics did not exceed the Target Values and showed that trace elements were mainly present in the fine fraction of <150 μm. The oxidation of sulphide minerals such as pyrite resulted into the elevated concentration for all nourishment sites, especially when an unsaturated zone was present and influence of rainwater was apparent. To prevent trace metal mobility at a mega beach nourishment it is important to retain seawater influences and limit oxidation processes. In this respect, a shoreface nourishment is recommended rather than a mega beach nourishment with a thick unsaturated zone. Consequently, we conclude that whether a site is carbonate-rich or carbonate-poor is unimportant, as the influence of seawater will prevent decalcification, creating a low risk of mobilisation of trace elements.

© 2017 The Authors. Published by Elsevier Ltd. This is an open access article under the CC BY-NC-ND license (<http://creativecommons.org/licenses/by-nc-nd/4.0/>).

## 1. Introduction

Of the ice-free coastlines in the world, two-thirds consist of sandy beaches (Brown and McLachlan, 2006). With 60% of the human population living close to the shoreline, sandy beaches are extremely important for coastal zone management such as coastal protection and recreation. Therefore, when a beach becomes too narrow for protection or recreation, beaches are usually replenished with sand. This procedure is called beach nourishment. In the Netherlands, beach nourishments are applied to diminish the possibility of seawater flooding, whereas in Spain nourishments

serve recreational purposes (Hanson et al., 2002). Often neglected at a beach is nature development. Sandy beaches are generally likened to marine deserts, but research has shown that they contain interesting and often productive ecosystems and add to the diversity of a coastal area (Brown and McLachlan, 2006).

Environmental studies of beaches mainly focus on environmental chemistry, both organic (Benlahcen et al., 1997; Moreira et al., 2016) and inorganic (Alshahri, 2017; Vetrimurugan et al., 2017). Most of these studies investigate contamination from industrial activity (e.g. Foteinis et al., 2013; Lafabrie et al., 2008). The environmental consequences of beach nourishments are generally researched from an ecological perspective, such as the effect of volume and grain size distribution on the survival of benthic communities (Post et al., 2017; Van Dalen and Essink, 2001). Toxic substances such as trace elements, polycyclic aromatic hydrocarbons (PAHs) and polychlorinated biphenyls (PCBs) are regarded as

<sup>☆</sup> This paper has been recommended for acceptance by Yong Sik Ok.

\* Corresponding author.

E-mail address: [i.r.pit@uu.nl](mailto:i.r.pit@uu.nl) (I.R. Pit).

an important quality criterion (Speybroeck et al., 2006), especially in relation to human health risks where, for example, high concentrations of arsenic can be a hazard if children use the beaches for recreation (Van Bruggen et al., 2014). Trace element bonding on solid compounds is a critical factor for mobility and bioavailability. While dissolved or weakly bound adsorbed trace elements may be available to plants and aquatic organisms, trace elements bound in the crystalline structural lattice of minerals are not available to biota, except when these minerals undergo chemical weathering (Calmano et al., 1993). Most beach studies have neglected chemical processes that may increase the solubility and potential bioavailability of trace elements (Bruce, 1928; El-Kammar et al., 2007; Stuyfzand et al., 2012).

Traditional beach nourishments are periodic sand replenishments that are regarded as an environmentally acceptable method of coastal management (Hanson et al., 2002). Innovative coastal management that also takes natural processes into account has recently been introduced in the Netherlands under the 'Building with Nature' paradigm (De Vriend and Van Koningsveld, 2012). Within this context, the Sand Engine concept, developed in the Netherlands, is the first project to combine coastal engineering with environmental, ecological and social considerations (Stive et al., 2013). The Sand Engine is a 21.5 million m<sup>3</sup> mega beach nourishment applied along the Dutch coast in 2011, which is an artificial sand spit rising to 6 m above mean sea level and was shaped like a large hook, with an initial length of 2.4 km and a width of 1 km that extends offshore. The environmental, ecological and social consequences of such a mega beach nourishment still have to be evaluated before the approach can be unrolled in other locations.

Beach nourishments along the Dutch coast consist of geological sediments dredged from the sea floor. During the construction, the environmental conditions of the sediments used change from anaerobic to aerobic. As a result, chemical weathering processes are encouraged, by oxygen, carbon dioxide and other acidic components, including atmospheric deposition, causing primary minerals to break down chemically into secondary minerals and release dissolved elements to natural waters (Salbu and Steinnes, 1994). In the Sand Engine mega beach nourishment, Pit et al. (2017) found two geochemical processes dominant: pyrite oxidation and freshening. Oxidation of pyrite, one of the most abundant sulphide minerals, may mobilise metals and metalloids that can be incorporated or sorbed to the mineral (Smith and Melville, 2004). Both pyrite oxidation and freshening processes enhance calcite dissolution, which over time may decrease pH and potentially dissolve trace elements. Besides oxidation and freshening, physical sorting processes may cause higher values to occur locally in fine sediments, which potentially may enrich these sites with iron oxides and trace elements (Pit et al., 2017).

Due to an environmental change of beach nourishment material from anoxic to oxic, the reactive minerals may change from metal sulphides to carbonates or oxyhydroxides where the solubility of trace elements is changed and controlled by adsorption to Mn and Fe oxyhydroxides and organic matter if present (Salbu and Steinnes, 1994). For metal cations such as Pb, Cu and Cd, adsorption is high under pH neutral or slightly alkaline conditions (Langmuir, 1997), which is typical for a marine environment. Oxyanions like As, Cr and Mo are weakly dependent on the pH and achieve maximum release in the neutral pH range (Paoletti, 2002). Calmano et al. (1993) found that at identical pH values, Cd and Zn concentrations are more mobilised in oxidised sediment than in anaerobic sediment, which according to Shaheen and Rinklebe (2017) may be connected to changes of controlling factors such as dissolved organic carbon (DOC), Fe, Mn and SO<sub>4</sub><sup>2-</sup>. As freshening may occur in oxic beach nourishment material (Pit et al., 2017), a

decline in pH as a result of rainwater infiltration can affect the mobility of trace elements (Stumm and Morgan, 2012). Other controlling factors like DOC or a dynamic E<sub>h</sub> (Frohne et al., 2011), are expected to be unimportant at beach nourishments, because of its generally oxic environment with relatively coarse sand and low turnover of organic matter.

We set out to understand the main factors that control the mobilisation of toxic trace elements at a beach nourishment. Both surface sediment chemistry and pore water chemistry were compared at four different sites along the Dutch coast: two traditional beach nourishment sites, one mega beach nourishment site and, as a reference, a natural beach. Our hypothesis is that if pyrite is present and exposed to air, pyrite oxidation will be the main contributor to the mobilisation of toxic trace elements at beach nourishments. Freshening is expected to decrease the pH of beach nourishments in time, which will further enhance the mobilisation of trace elements. With the mega beach nourishment having the largest volume of nourishment material above sea level, we expect that this site will show the highest mobilisation of toxic trace elements compared to the traditional beach nourishments. Additionally, pyrite and therefore possible pyrite oxidation at the reference site is most likely present in low amounts compared to the three beach nourishments, because of the gradual, natural growth of this coast line.

## 2. Materials and methods

### 2.1. Sampling

We compared four sites along the Dutch coast (Fig. 1), two of which are in a carbonate-rich environment (>2% CaCO<sub>3</sub>), and two in a carbonate-poor environment (<0.5% CaCO<sub>3</sub>) (Eisma, 1968). Beach and dune sand along the Dutch coast show a transition in CaCO<sub>3</sub> content and becomes less calcareous northwards. The transition of carbonate content is near Bergen (Baak, 1936; Eisma, 1968).

The first site is the Sand Engine pilot project, a mega beach nourishment (Stive et al., 2013). The Sand Engine is a locally concentrated sand nourishment constructed in 2011 from 21.5 million m<sup>3</sup> of sand in a carbonate-rich environment (Megar). To construct the Sand Engine, material was dredged from a sand pit 10 km offshore to a maximum depth of 6 m below the sea floor (Fiselier, 2012). The dredged material is both Holocene and Pleistocene in origin (Pit et al., 2017). The second site is a traditional beach nourishment in the southernmost part of the Dutch coast where the coastline is carbonate-rich (Trad<sub>R</sub>). The beach nourishment was also applied in 2011 and contains a volume of 0.7 million m<sup>3</sup> spread out across the total width of a 3.4 km long stretch of beach. The offshore area from which the sand was obtained from was dredged to a depth of 2 m. The third and fourth sites are in the northern coastal area where beaches and dunes are carbonate-poor. One is a traditional beach nourishment at the northern end of the western coastline (Trad<sub>P</sub>). This beach nourishment was constructed in 2011 and also contains 0.7 million m<sup>3</sup> over a stretch of 4.7 km. The sand pit from which the sand was retrieved was dredged to a depth of 2 m. The fourth and last site, our reference site, is on a Wadden island and consists of a natural beach of carbonate-poor sand without human interference (Ref<sub>P</sub>).

Fieldwork was carried out in summer and autumn 2014. At each of the four sites, samples were taken during low tide of both surface sediment and pore water via multiple transects with sampling points at the high water line, in the middle of the beach and close to the dune ridge (see Fig. 1). At every point in the transect around 500 g of surface sand was sampled by mixing five subsamples. Pore water was collected from samples taken at 50 cm depth. A hole 50 cm deep was drilled with an Edelman auger. Next, an

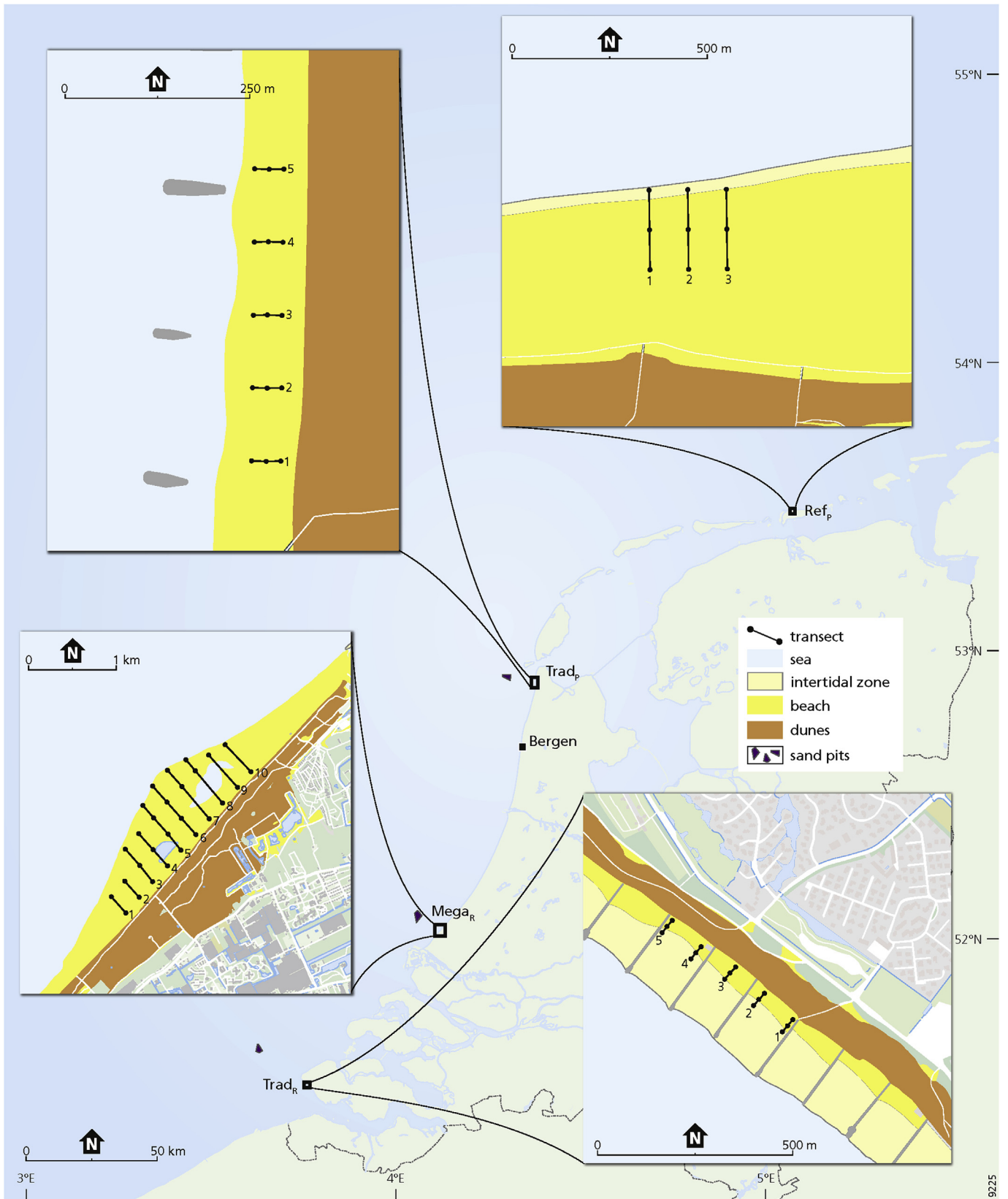


**Fig. 1.** The locations of the sampling sites. The carbonate-rich mega beach nourishment (Mega<sub>R</sub>), the traditional beach nourishments in the carbonate-rich (Trad<sub>R</sub>) and the carbonate-poor (Trad<sub>P</sub>) areas of the Dutch coast and the carbonate-poor reference location (Ref<sub>P</sub>).

undisturbed sand sample was taken from the bottom of the hole in a Ø38 × 240 mm stainless steel core with an Akkerman core sampler. Pore water was immediately extracted from the core by using a rhizon (Seeberg-Elverfeldt et al., 2005). If there was insufficient soil moisture, a rhizon could not be used and pore water had to be extracted in the lab. The cores were transported to the lab in a cooler at temperatures comparable to those at the field site. The sediment from a core was placed in a plastic centrifuge bottle with a 0.45 µm filter at the bottom and a reservoir below for the pore water, and the bottle was centrifuged for 30 min at 2000 rpm.

## 2.2. Chemical analyses

Chemical analyses were performed on both pore water and sand samples. The pore water was analysed for anions using ion chromatography and inductively coupled plasma mass spectrometry (ICP-MS) for metals. Within 24 h after sampling, the alkalinity as HCO<sub>3</sub><sup>-</sup> was measured using the Gran titration method (Stumm and Morgan, 2012) and the pH was determined with an Orion 520A-pH meter.

The sand samples were dried in the oven at 105 °C for at least 24 h. Grain size distribution was measured with a laser diffraction analyser (Malvern Instruments Ltd., 1998) commonly without pre-treatment. Only the samples from the Megar were pre-treated in accordance with NEN 5753 (1990) to reduce aggregation of the soil particles. A total of 15 samples were both pre-treated and untreated. When both pre-treated and untreated samples were measured for grain size distribution, no significant differences were found, probably because of the low contents of organic matter and clay in the sand samples.

Following Pit et al. (2017), sand samples were sieved to obtain two fractions: < 150 µm (100 mesh) and 150–2000 µm (10–100 mesh), where the latter fraction was ground to < 2 µm. Both fractions were analysed for total C and S contents with the CS elemental analyser. To obtain the thermogravimetric analysis (TGA) for quantitative determination of mineral compounds, the sand fractions were heated from 25 to 1000 °C at a heating rate of 1 °C/min, using a Leco TGA-601. The aqua regia digestion method (Houba et al., 1995) was used to obtain the pseudo-total elemental concentrations (Chen and Ma, 2001), which were analysed with inductively coupled plasma optical emission spectrometry (ICP-OES) and mass spectrometry (ICP-MS) to obtain similar main and trace elements as in the pore water.

The measured concentrations in sand and pore water were compared to Dutch Quality Standards (Qs) for soil and groundwater (Swartjes et al., 2012). The framework is described in the Ministerial Circular on Soil Remediation (VROM, 2009) which is a supplement to the Dutch Soil Protection Act. There are two types of generic Qs, namely the Target Values (the values at which there is a sustainable soil quality) and the Intervention Values (the threshold above which the soil's functions for people, vegetation and benthos are at risk) (Lijzen et al., 2001). Application of Target Values and Intervention Values results in a classification of either 'clean soil', 'slightly contaminated soil' or 'seriously contaminated soil' (Swartjes et al., 2012).

## 2.3. Statistical analyses

Data analyses were performed on the pore water and sediment data sets and consisted of the Wilcoxon rank sum test (R software: Ihaka and Gentleman, 1996), to test whether the locations differed significantly from each other (Wilcoxon, 1945). Following Reimann et al. (2011), the data set was prepared by replacing values below the detection limit with a value half of that detection limit. As more than 25% of the aquatic samples were below the detection limit for

Al, Cd, Fe, NO<sub>2</sub> and Pb, they were excluded from the data analyses.

For the multivariate statistical data analyses the focus was on the pore water data set, because chemical species are more readily bioavailable in the pore water than in the sediment (Stumm and Morgan, 2012). All variables were ratio transformed using the isometric log-ratio (ilr) transformation (Egozcue et al., 2003). This transformation is generally preferred over a normal log-ratio transformation for environmental data since it generates a robust estimation of the covariance matrix (Filzmoser et al., 2009). The ilr-transformed data was then back-transformed to centred log-ratio (clr) space to maintain the links to the original variables and enable direct interpretation.

A correlation matrix of the pore water data set was created between the trace elements As, Cr, Cu Ni, Mo and Zn, and the main solutes such as Cl, SO<sub>4</sub> and HCO<sub>3</sub><sup>-</sup>, to detect possible linkages between trace elements, seawater content and alkalinity. Then, for multidimensional scaling and to combine sediment properties with pore water chemistry, an unconstrained principal component analysis (PCA) was performed on the pore water data set with supplementary variables, using the Canoco 5 program (Braak and Šmilauer, 2012). With the unconstrained PCA, variation in aqueous composition was presented in an ordinogram combined with the following supplementary variables: pH, sedimentary S content, CaCO<sub>3</sub> content, Δm<sub>SO<sub>4</sub></sub> (see next paragraph), fraction < 150 µm and relative distance to the sea.

## 2.4. Pyrite oxidation

To elucidate whether pyrite oxidation had occurred at the four different sites, the measured SO<sub>4</sub> concentration was compared with the composition for conservative mixing of fresh water and seawater. The fraction of seawater (*f<sub>sea</sub>*) was calculated from the Cl concentration (Appelo and Postma, 2005):

$$f_{sea} = \frac{m_{Cl, sample} - m_{Cl, fresh}}{m_{Cl, sea} - m_{Cl, fresh}} \quad (1)$$

where *m<sub>Cl, sample</sub>* is the Cl concentration of the sample, *m<sub>Cl, fresh</sub>* the Cl concentration in rainwater and *m<sub>Cl, sea</sub>* the concentration in seawater. The conservative mixing concentration (*m<sub>SO<sub>4</sub>, mix</sub>*) is calculated from:

$$m_{SO_4, mix} = f_{sea} \cdot m_{SO_4, sea} + (1 - f_{sea}) \cdot m_{SO_4, fresh} \quad (2)$$

where *m<sub>SO<sub>4</sub>, sea</sub>* and *m<sub>SO<sub>4</sub>, fresh</sub>* are the concentrations of SO<sub>4</sub> in seawater and fresh water, respectively. The aqueous composition of rainwater was derived from Stolk (2001) with 2.4 ppm SO<sub>4</sub> and that of seawater from Hem (1985) with 2700 ppm SO<sub>4</sub>. The enrichment or depletion of SO<sub>4</sub> (Δ*m<sub>SO<sub>4</sub></sub>*) is then obtained by:

$$\Delta m_{SO_4} = m_{SO_4, sample} - m_{SO_4, mix} \quad (3)$$

A positive Δ*m<sub>SO<sub>4</sub></sub>* indicates pore water is enriched with SO<sub>4</sub> and this enrichment is most likely associated with oxidation of sulphide minerals such as pyrite; a negative Δ*m<sub>SO<sub>4</sub></sub>* indicates SO<sub>4</sub> has been depleted, which may be the result of SO<sub>4</sub> reduction.

## 2.5. Time calculations

Buffering capacity of the sediment for pH is an important factor affecting the mobility of trace elements and the time needed to decrease the buffering capacity depends strongly on the amount of CaCO<sub>3</sub> and on geochemical processes such as freshening and pyrite oxidation. We used the PHREEQC program (Parkhurst and Appelo, 2013) to estimate the amount of CaCO<sub>3</sub> that may dissolve per 0.5

vertical metre of sand (per  $\text{dm}^2$  surface area) at a typical carbonate-rich site and at a typical carbonate-poor site. Based on earlier findings (Pit et al., 2017), we assumed that the system is open to atmospheric gas exchange, with the partial pressure of  $\text{CO}_2$  ( $P_{\text{CO}_2}$ ) in the pore water of Mega<sub>R</sub> to be a minimum of  $10^{-3.66}$  atm and thus close to the average  $P_{\text{CO}_2}$  of the atmosphere ( $10^{-3.5}$  atm).

Two opposing scenarios were investigated of a 0.5 m sand profile with a porosity of 40%: one in which the sand is only affected by seawater during every spring tide and the other where only rainwater infiltrates the sand. The first scenario assumes that the sand remains 20% saturated with seawater and is flooded during spring tides. During spring tide water will rise until maximum 1.5 m above mean sea level. The investigated sand profile lies above high tide and during spring tide a 'worst-case scenario' is created: a seawater wetting front of 0.5 m will be available to infiltrate into the sand profile during a spring tide and replace the water 5 times because of the 20% saturation. With a spring tide occurring every 14 days, the sand profile will be flushed 130 times with seawater per year. The second scenario was calculated with the 1990–2015 average annual precipitation and evaporation in order to estimate the precipitation surplus: 271 mm per year (CBS et al., 2016). The scenario assumes relatively dry sand with a water content of 10% in the first 0.5 m of the sand profile; as a result, this water will be replaced with rainwater 5.42 times per year as the precipitation surplus coincides with  $2.71 \text{ dm}^3$  of water per  $\text{dm}^2$  surface area.

### 3. Results

Below, the sediment characteristics of the different sites are compared, including their grain size distribution, followed by the chemistry of the pore water. Next, correlations are shown between sediment and pore water chemistry. Finally, extrapolations in time are made to calculate how long the systems will remain pH buffered.

#### 3.1. Sediment characteristics

Fig. 2 shows the average grain size distribution of the four different sites. The reference location clearly shows finer grain size distribution ( $D_{50}$  of  $215 \mu\text{m}$  and 7% <  $150 \mu\text{m}$  fraction) than the three nourishment locations. Comparison of the nourishment locations reveals that Mega<sub>R</sub> has the coarsest grain size distribution with a  $D_{50}$  of  $378 \mu\text{m}$  and a <  $150 \mu\text{m}$  fraction of 2%. The Mega<sub>R</sub> also has poorer sorting than the traditional nourishments. The two traditional nourishments show a very similar grain size distribution despite the different dredging locations, with Trad<sub>R</sub> showing a  $D_{50}$  of  $361 \mu\text{m}$  and a <  $150 \mu\text{m}$  fraction of 0.2%, and Trad<sub>P</sub> a  $D_{50}$  of  $356 \mu\text{m}$  and a <  $150 \mu\text{m}$  fraction of 0.1%.

Table 1 shows the general chemistry of both the total sediment and the fine fraction (<  $150 \mu\text{m}$ ). Overall, Mega<sub>R</sub> differs significantly from the other sites. The high median absolute deviation (MAD) values of Mega<sub>R</sub> compared to the traditional nourishments may be related to the fact that Mega<sub>R</sub> has source material from two different geological layers, whereas the traditional nourishments are more likely to contain material from one geological layer only. Trad<sub>R</sub> and Trad<sub>P</sub> share similar characteristics, especially in the fine fraction. For the traditional nourishments, the sand was dredged to 2 m depth, whereas for Mega<sub>R</sub> it was dredged to 6 m depth. Large heterogeneity is also visible for the reference site and is probably related to the larger contribution of the fine fraction (see in Fig. 2), which can influence the total elemental content.

Mega<sub>R</sub> and Trad<sub>R</sub> are in the carbonate-rich part of the coastal zone of the Netherlands and both were found to have a >2%  $\text{CaCO}_3$  content, with median 3.9% for Mega<sub>R</sub> and 2.3% for Trad<sub>R</sub>, whereas Trad<sub>P</sub> and Ref<sub>P</sub>, located in the carbonate-poor part of the coastal

zone, had  $\text{CaCO}_3$  contents of 1.0% and 1.3%, respectively. The highest carbonate content in the total sediment was observed in Mega<sub>R</sub>, but here the lowest carbonate content was found in the fine fraction. Apparently,  $\text{CaCO}_3$  is more abundant in the coarse fraction at the Mega<sub>R</sub>, whereas the opposite is the case for Ref<sub>P</sub>; this may confirm the geological differences between these sites. The findings of Eisma (1968) show that the differences in  $\text{CaCO}_3$  content between the carbonate-rich and carbonate-poor coastline are predominantly due to variations in the distribution of shell fragments in the coarse fraction and detrital calcite grains in the fine fraction.

The presence of sulphur indicates the likelihood of pyrite oxidation as gypsum usually does not play a role in Dutch environments (Griffioen et al., 2016). Even though the concentrations of S do not differ greatly, the differences between the sites are significant, with the lowest content found at Mega<sub>R</sub>, whereas the amount of Fe bearing minerals at Mega<sub>R</sub> is significantly higher than at the other two traditional nourishments. This may be related to differences in geological formation, as found during a previous study of the Sand Engine (Pit et al., 2017).

The heavy mineral related element Ti shows very large variation, especially between the reference site and the nourishment sites. To better understand the differences between the sites, we plotted Al against Ti for the fine and the coarse fractions (Fig. 3). Although Al and Ti do not dissolve completely with the aqua regia destruction method, geological interpretations can be made, as most heavy minerals are stable minerals (Morton, 1984). Apparently, Ti shows a high content in the fine fraction for Ref<sub>P</sub>, Trad<sub>P</sub> and Trad<sub>R</sub> and a low content in Mega<sub>R</sub>, whereas in the coarse fraction the opposite is visible: the Ti content is high for Mega<sub>R</sub> and low for Ref<sub>P</sub>, Trad<sub>P</sub> and Trad<sub>R</sub>.

Table 2 shows the median and MAD values of the most important trace elements in the sediments. The Intervention Value is given and corrected from a standard soil with 10% organic material and 25% lutum (soil particles <  $2 \mu\text{m}$ ) to a soil most comparable to sand, with 2% organic material and 2% lutum (VROM, 2009). The trace element contents are low for all sites and the Intervention Values are not exceeded. Mega<sub>R</sub> again differs most significantly from the other sites, and Trad<sub>R</sub> and Trad<sub>P</sub> are very similar, as are Ref<sub>P</sub> and Trad<sub>P</sub>. No specific site has the highest contents for all trace elements. Values in the fine sediment fraction are higher than in the total sediment; the Intervention Value of Cr is on average often exceeded and the Intervention Value for Ni is exceeded for Trad<sub>P</sub>. Although the fraction of <  $150 \mu\text{m}$  is too small to contribute significantly to the overall content, it shows that most trace element content is present in the fine fraction.

#### 3.2. Pore water chemistry

Table 3 shows the general characteristics of the pore water in terms of pH, alkalinity,  $\text{SO}_4$  and Cl, together with the trace element concentrations. Mega<sub>R</sub> has a median Cl concentration of 169 ppm, which can be classified as fresh, whereas the other locations are in general more saline. Similar conclusions can be drawn from the  $\text{SO}_4$  concentration, which is high in saline water. The variation in pH between the sites is generally small, but Mega<sub>R</sub> shows the highest value and Trad<sub>P</sub> the lowest. A similar variation is seen for the  $\text{HCO}_3$  concentration, but here Mega<sub>R</sub> shows the lowest median concentration.

To estimate whether oxidation processes had influenced the aquatic samples, the concentrations of  $\text{SO}_4$  were plotted against Cl together with a mixing line of rainwater and seawater (Fig. 4). When  $\text{SO}_4$  concentrations are present above the mixing line, oxidation processes such as pyrite oxidation are causing elevated  $\text{SO}_4$  concentrations, whereas  $\text{SO}_4$  concentrations below the mixing line indicate reduction processes. Fig. 4 shows that elevated  $\text{SO}_4$

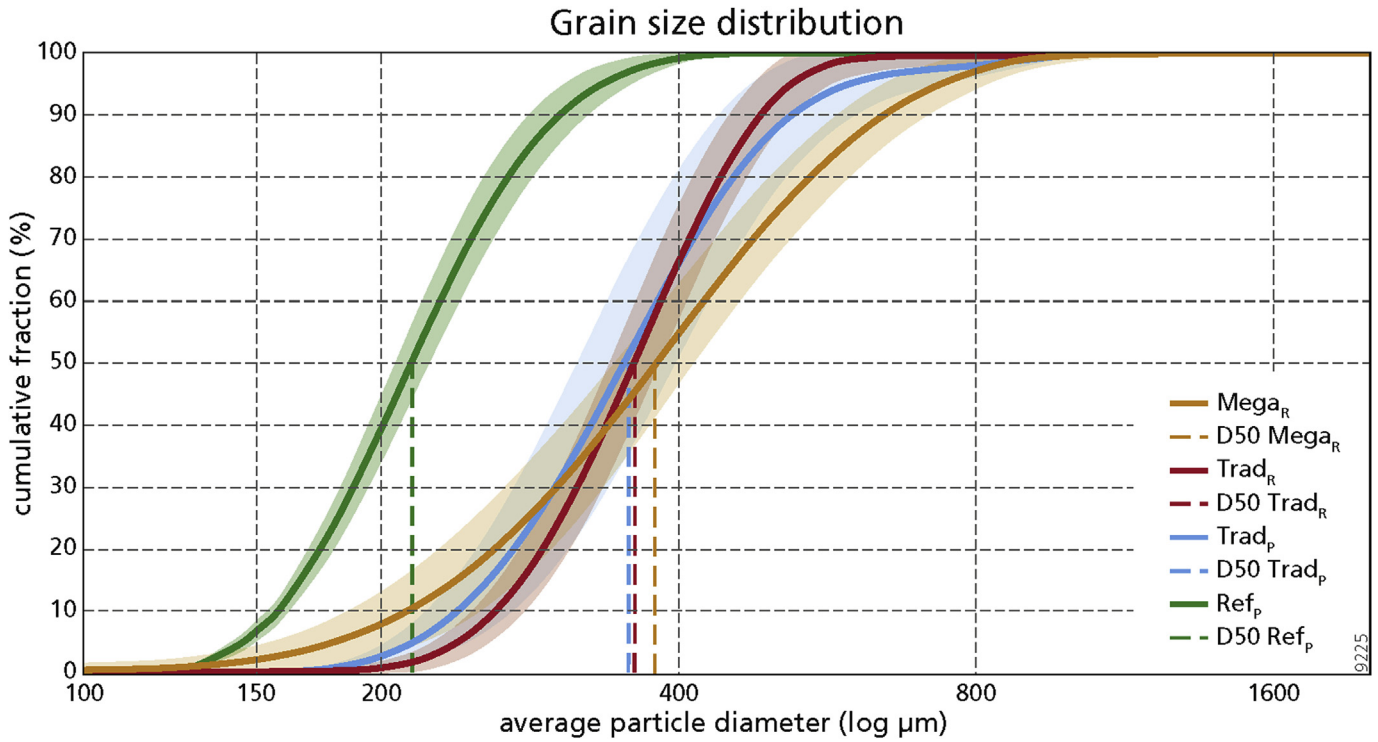


Fig. 2. The average grain size distribution of the four different sites, including the D50.

**Table 1**  
Median results of CaCO<sub>3</sub>, S, Fe, Al and Ti of total sediment and fine fraction (<150 μm) including the MAD (Median Absolute Deviation, which is similar to the Standard Deviation but where the central value is the median instead of the mean). Sites that show a significant difference (p < 0.05) are listed with a different letter.

		n	Median (MAD) significance				
			CaCO <sub>3</sub> (%)	S (ppm)	Fe (ppm)	Al (ppm)	Ti (ppm)
Total Sediment	Mega <sub>R</sub>	28	3.9 (1.8) d	624 (152) a	3618 (1002) c	2280 (499) c	171 (64) b
	Trad <sub>R</sub>	15	2.3 (1.1) c	740 (24) b	2174 (391) b	1228 (240) a	51.5 (38) a
	Trad <sub>P</sub>	15	1.0 (0.4) a	780 (23) c	1844 (324) a	1365 (295) b	50.1 (42) a
	Ref <sub>P</sub>	9	1.3 (0.7) b	873 (66) d	3260 (1230) c	2448 (514) c	758 (285) c
Fine Fraction	Mega <sub>R</sub>	28	2.4 (6.5) a	n.a.	11900 (3054) a	4322 (722) a	1357 (616) a
	Trad <sub>R</sub>	15	3.1 (3.0) b	756 (19) ba	21250 (4020) c	6784 (1892) b	5198 (2055) b
	Trad <sub>P</sub>	15	3.5 (4.0) b	777 (56) b	19000 (18140) bc	6913 (2623) b	3060 (3465) b
	Ref <sub>P</sub>	9	13.8 (0.2) c	746 (34) a	14710 (4543) ab	5938 (674) b	5731 (984) b

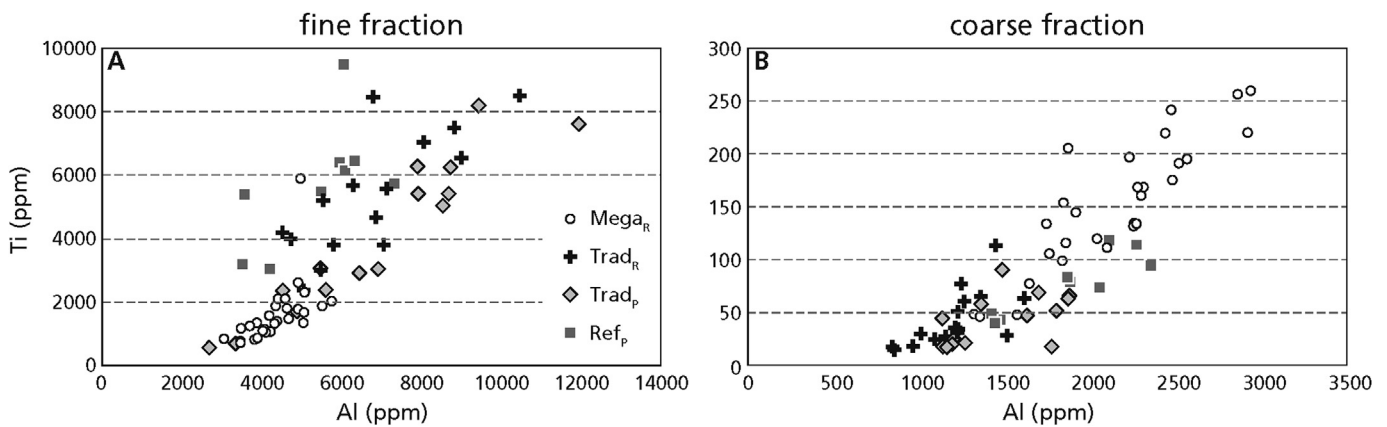


Fig. 3. Correlations between Al and Ti contents of samples for both the fine (<150 μm) and coarse (150–2000 μm) fractions.

**Table 2**

Median contents (in ppm) results for trace metals As, Cd, Cr, Cu, Pb, Ni, Mo and Zn of total sediment and fine fraction (<150 μm) including the MAD (Median Absolute Deviation). Sites that show a significant difference (p < 0.05) are listed with a different letter. Intervention values for standard Dutch soil with 10% organic material and 25% lutum (soil particles < 2 μm) are corrected for a soil with maximum 2% organic material and 2% lutum (VR0M, 2009).

	n	Median (MAD) significance								
		As	Cd	Cr	Cu	Pb	Ni	Mo	Zn	
Intervention value		44	8	42	92	337	12	190	303	
Total Sediment	Mega <sub>R</sub>	28	2.8 (0.8) a	0.02 (0.01) a	8.3 (2.7) a	0.6 (0.3) a	2.7 (0.4) c	5.1 (1.2) c	0.07 (0.02) a	8.1 (2.4) ab
	Trad <sub>R</sub>	15	4.1 (1.0) b	0.07 (0.03) b	4.3 (1.1) b	1.9 (0.5) c	1.9 (0.2) a	1.7 (0.3) a	0.17 (0.07) b	6.9 (1.5) a
	Trad <sub>P</sub>	15	2.7 (0.3) a	0.09 (0.04) bc	4.2 (2.0) b	1.5 (0.1) c	2.3 (0.3) b	2.3 (0.4) b	0.13 (0.02) b	7.9 (0.8) b
	Ref <sub>P</sub>	9	2.5 (0.5) a	0.14 (0.01) c	9.9 (5.8) a	1.1 (0.1) b	3.4 (0.9) d	2.2 (0.4) b	0.13 (0.02) c	7.9 (1.8) b
Fine Fraction	Mega <sub>R</sub>	28	6.4 (1.5) a	0.08 (0.02) a	36.6 (12.8) a	7.8 (1.3) c	4.0 (1.2) a	8.9 (1.2) c	0.2 (0.1) a	19.3 (4.4) a
	Trad <sub>R</sub>	15	15.1 (6.8) c	0.30 (0.04) c	90.4 (33.5) b	1.9 (0.3) b	13.9 (5.9) b	7.3 (2.5) b	0.6 (0.2) c	23.1 (6.7) b
	Trad <sub>P</sub>	15	7.4 (5.4) b	0.10 (0.03) b	171 (165) b	1.9 (1.3) b	10.1 (8.8) b	11.7 (7.0) c	0.5 (0.2) c	31.4 (17.9) b
	Ref <sub>P</sub>	9	7.3 (3.2) ab	0.09 (0.03) b	56.6 (33.5) a	1.0 (0.5) a	13.7 (4.1) b	4.8 (0.9) a	0.3 (0.2) b	21.8 (8.5) ab

**Table 3**

Median results for trace metals As, Cd, Cr, Cu, Pb, Ni, Mo and Zn of pore water, including the MAD (Median Absolute Deviation: similar to the SD, but with the median as central value) given in brackets. Sites that show a significant difference (p > 0.05) are listed with a different letter and the lowest median starts with the letter 'a'. Not available (n.a.) is shown in the Table when more than 25% of the results were below detection limit. Target and intervention values are for shallow groundwater (VR0M, 2009). The intervention values were barely exceeded\* and therefore not visible in the Table.

n	pH	HCO <sub>3</sub> <sup>-</sup> (ppm)	SO <sub>4</sub> (ppm)	Cl (ppm)	As (ppb)	Cd (ppb)	Cr (ppb)	Cu (ppb)	Pb (ppb)	Ni (ppb)	Mo (ppb)	Zn (ppb)	
													Median (MAD) significance
Mega <sub>R</sub>	28	8.4 (0.4) b	151 (57) a	104 (77) a	169 (195) a	2.6 (1.5) a	n.a.	2.0 (1.5) ab	4.7 (3.0) ab	n.a.	4.9 (5.0) a	6.6 (4.2) a	5.0 (3.7) a
Trad <sub>R</sub>	15	8.1 (0.5) ab	160 (15.5) ab	1160 (1618) b	8169 (11640) b	5.0 (3.0) b	n.a.	2.3 (1.4) b	5.7 (4.3) ab	n.a.	16.9 (6.2) b	13.7 (2.0) bc	10.0 (3.0) b
Trad <sub>P</sub>	15	7.8 (0.2) a	172 (34.4) b	1932 (901) b	12580 (6865) b	4.1 (2.5) b	0.12 (0.14) b	1.5 (0.8) b	5.6 (3.0) b	n.a.	13.0 (2.1) b	12.7 (2.2) b	11.0 (4.4) b
Ref <sub>P</sub>	9	7.9 (0.2) ab	193 (50.2) ab	1087 (1199) b	7974 (8672) b	4.2 (1.0) ab	n.a.	0.6 (0.1) a	3.7 (0.4) a	n.a.	7.8 (5.3) a	8.4 (3.7) ac	6.0 (4.4) a
Target value					10	0.4	1	20	15	15	5	65	
Mega <sub>R</sub>		> target value			11%		43%	11%	11%	11%	68%	7.1%	
Trad <sub>R</sub>		> target value			33%		73%		53%	80%			
Trad <sub>P</sub>		> target value			33%	20%	73%	13%	20%	93%	20%		
Ref <sub>P</sub>		> target value					22%		22%	78%			

\*The intervention values were exceeded once for As (Trad<sub>R</sub>), Cr (Mega<sub>R</sub>) and Zn (Trad<sub>P</sub>).

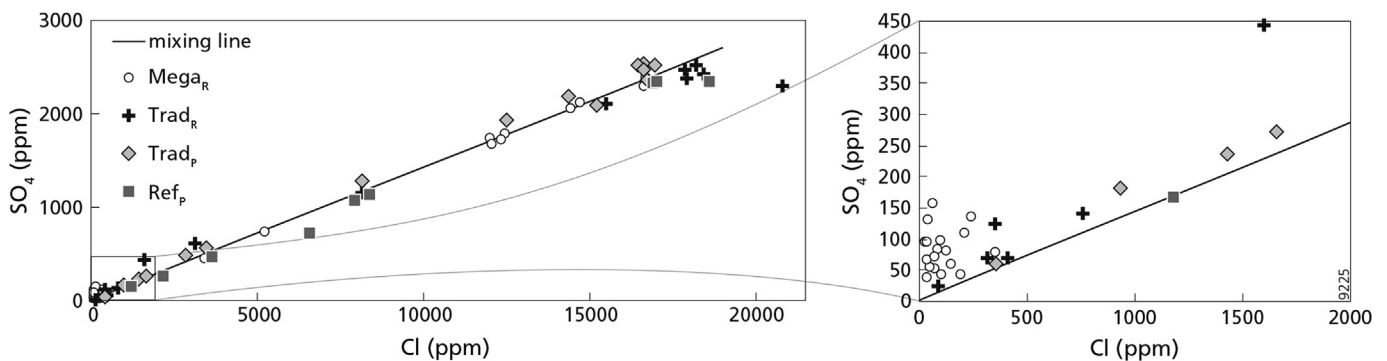


**Fig. 4.** Concentrations of SO<sub>4</sub> versus Cl for the pore water samples, including a close-up (right-hand panel) with the mixing line of rainwater and seawater.

concentrations are mainly present in the low Cl range, 0–2000 ppm, and that as Cl concentration increases, SO<sub>4</sub> reduction processes become dominant, with many SO<sub>4</sub> concentrations below the mixing line at Cl concentrations above 15,000 ppm. Close to the water line, the seawater fraction is high and the sand profile more permanently saturated, which may result in reducing conditions, whereas in the higher parts of the beach, where a thick unsaturated zone is present, oxidation of sulphide minerals can occur with infiltration of rain water.

The Δm<sub>SO<sub>4</sub></sub> is –66 to 146 ppm at Mega<sub>R</sub>, –662 to 215 ppm at

Trad<sub>R</sub> and –71 to 175 ppm at Trad<sub>P</sub>. At Ref<sub>P</sub> only reducing conditions are seen with a Δm<sub>SO<sub>4</sub></sub> of –303 to –1 ppm. Dividing the Cl concentrations into the low Cl range (0–2000 ppm) and high Cl range (>2000 ppm) reveals large differences between the sites in their SO<sub>4</sub> concentrations relative to the mixing line. The low Cl range shows overall oxidation processes with a median Δm<sub>SO<sub>4</sub></sub> of 61 ppm at Mega<sub>R</sub>, followed by Trad<sub>P</sub> with a median of 36 ppm and Trad<sub>R</sub> with a median of 27 ppm. At Ref<sub>P</sub> there is only one sample in the low Cl range with a Δm<sub>SO<sub>4</sub></sub> of 1 ppm. For the saline range (high Cl), the Δm<sub>SO<sub>4</sub></sub> is still positive (with 9 ppm) at Mega<sub>R</sub> indicating

pyrite oxidation. It is even higher at Trad<sub>P</sub> (by 123 ppm), whereas at the other two sites it is negative: –90 ppm at Trad<sub>R</sub> and –80 ppm at Ref<sub>P</sub>. As the sedimentary S concentrations do not differ very much from each other,  $\Delta m_{SO_4}$  gives an indication of the aeration of the sand and the amount of S minerals such as pyrite that may oxidise. Summarising, Mega<sub>R</sub> shows the highest pyrite oxidation present in the low Cl range, whereas Trad<sub>P</sub> shows the highest pyrite oxidation in the saline range.

The trace element concentrations in pore water varied much more than the sediment characteristics: Mega<sub>R</sub> and Ref<sub>P</sub> are largely similar, as are Trad<sub>P</sub> and Trad<sub>R</sub>. Table 3 gives the results and compares them with the Target Values and Intervention Values for trace metals in shallow groundwater (VROM, 2009). The Target Values are often exceeded for Cr, Ni and Mo and to a lesser extent for As. The Intervention Value is barely exceeded: As, Cr and Zn each have one anomalous sample in which the concentration is high. Both Cd and Pb are often below detection limit.

To gain more information about the differences and similarities between the sites, a correlation matrix was created for the trace elements As, Cr, Cu, Ni, Mo, Zn and the major ions SO<sub>4</sub>, Cl and HCO<sub>3</sub> (Fig. 5). The Cl concentration, which is an indicator of seawater fraction, correlates strongly with trace element concentrations. Negative correlations with Cl of –0.60 or lower are seen for As (–0.63), Cr (–0.87), Cu (–0.8) and HCO<sub>3</sub> (–0.71), while the positive correlation with SO<sub>4</sub> (0.91) is because seawater has a much higher SO<sub>4</sub> concentration than rainwater. Consequently, the strong negative correlations of As, Cr, Cu and HCO<sub>3</sub> are also seen with SO<sub>4</sub>. A strong positive correlation is seen between the trace elements Cr and Cu (0.69). Negative correlations between trace elements and Cl and SO<sub>4</sub> show that fresh water generally has higher concentrations of As, Cr, Cu and HCO<sub>3</sub>. Fresh water can indeed increase HCO<sub>3</sub> concentration, as rainwater is slightly acidic and enhances calcite dissolution. Fresh water is present in the elevated parts of the nourishments where a (thick) unsaturated zone exists and oxidation affects the aquatic chemistry as well, whereas a high seawater content is present at the water line and the sand profile is close to aqueous saturation.

### 3.3. Links between sediment and pore water

To analyse whether the characteristics of pore water and sediment are linked, a PCA was performed on the chemical characteristics of pore water. Six supplementary variables were projected on this PCA: pH,  $\Delta m_{SO_4}$ , 150  $\mu\text{m}$  fraction, distance from the low water line, and sedimentary S and CaCO<sub>3</sub> contents. The PCA of the pore water chemistry shows a total explained variance of 90% divided over four different axes: the explained variance is 69% for the first axis, 10% for the second axis, 6% for the third axis and 5% for the fourth axis. Two of the four axes are presented in an ordination diagram with the sample locations, the aqueous solutes and the six supplementary variables (Fig. 6). In Fig. 6 the supplementary variables are shown with thick grey arrows and the aqueous solutes with black arrows. The ordination diagram shows the marginal effect of each supplementary variable upon the sample scores. The direction of the arrows indicates the steepest increase of the covariance of the supplementary variable with the aqueous solutes.

The supplementary variables pH and distance from the low water line both show a high response to the first axis (92% and 70% respectively) and to a lesser extent  $\Delta m_{SO_4}$  (39%), which means that with increasing distance from the sea, pH increases as well as  $\Delta m_{SO_4}$  indicating oxidation and this coincides with higher concentrations of Cr, Cu, NO<sub>3</sub>, Se and HCO<sub>3</sub> (Fig. 6). A strong negative response for the first axis is seen for sedimentary S (–51%); it is connected to Cl, Na and Br, indicating the presence of seawater and water-saturated conditions. Opposite from sedimentary S in the

ordination diagram and close to each other are the <150  $\mu\text{m}$  fraction and CaCO<sub>3</sub>, which show responses for the first axis of 20% and 59%, respectively. These variables show the highest positive response for the second axis: 20% (<150  $\mu\text{m}$  fraction) and 30% (CaCO<sub>3</sub>). The largest negative response is sedimentary S: –30%. What can be inferred from these variables is that sites that show a low seawater fraction are lower in sedimentary S, but higher in both <150  $\mu\text{m}$  fraction and CaCO<sub>3</sub> content with increased concentrations of Mn, Sb, Co and to a lesser extent of Zn. There seems no clear connection of a supplementary variable to the trace elements As, Mo, Ni and also V and P, which are strongly significant in the first and second axes in the PCA. As a result, trace elements seem less mobilised when a high seawater fraction and sedimentary S are present compared to a high distance from the sea where oxidation shows to increase the mobility of trace elements.

The sample locations, represented by different symbols in the ordination diagram, show that Mega<sub>R</sub> is dominant in the upper right corner of Fig. 6. Compared to the other locations it has the highest 150  $\mu\text{m}$  fraction and CaCO<sub>3</sub>, and pore water elements Co, Sb and Se. Also, the fact that the elements indicating seawater such as Cl and Na go in the opposite direction indicates that fresh water is predominant at Mega<sub>R</sub>, probably because of the altitude of the mega beach nourishment (6 m above mean sea level). The traditional nourishments are less high because less sand was used over a stretch of beach longer than at Mega<sub>R</sub>. The height of the sand at Mega<sub>R</sub> allows a freshwater lens to develop on top of the saline groundwater, resulting in fresh water dominating in the shallow groundwater.

In the lower right corner of the PCA, about half of the samples of Trad<sub>R</sub> and Trad<sub>P</sub> are seen and some samples of Mega<sub>R</sub>. These samples match the pore water elemental concentrations of HCO<sub>3</sub>, Cr and NO<sub>3</sub> and show that the alkalinity has increased at these sites together with high concentrations of Cr and NO<sub>3</sub>, but that the seawater contribution is low. Further, the two traditional nourishments (Trad<sub>R</sub> and Trad<sub>P</sub>) coincide with pore water elements V, As and P, indicating that whether the nourishment is located in a calcareous-rich or calcareous poor area is less important for possible oxidation processes connected to sulphide minerals such as pyrite which give rise to elevated concentrations of aquatic species such as As, P and V. Overall, Mega<sub>R</sub> is different from Trad<sub>R</sub> and Trad<sub>P</sub> in the diagram, which can be related to geological differences as Mega<sub>R</sub> consists of material originating from two geological layers (Pit et al., 2017), whereas the Trad<sub>R</sub> and Trad<sub>P</sub> most likely have material primarily from the Holocene.

Almost all samples from the Ref<sub>P</sub> and some from the other field sites are represented around aquatic species SO<sub>4</sub> and K, indicating the presence of seawater. Interestingly, the sample locations of Ref<sub>P</sub> are predominantly in the high saline range, which indicates that the sand profile in this natural beach has a thin unsaturated zone in which the influence of seawater is generally large. Ref<sub>P</sub> shows one location close to the supplementary variable  $\Delta m_{SO_4}$ , but lacks a clear connection to trace elements.

### 3.4. Estimating the depletion of buffer capacity with time

The carbonate buffer capacity prevents the pH from dropping to acidic conditions, which would otherwise result in less intensive sorption and higher concentrations of trace elements in the pore water. It is therefore interesting to know the time needed for all the CaCO<sub>3</sub> to dissolve when there is no artificial or natural replenishment of sand for prolonged period of time and the buffer capacity has finally disappeared.

The median CaCO<sub>3</sub> content is highest at Mega<sub>R</sub> (3.9%) and lowest at Trad<sub>P</sub> (1.0%). These two locations were used to estimate the amount of time required for all the CaCO<sub>3</sub> to go into solution. The



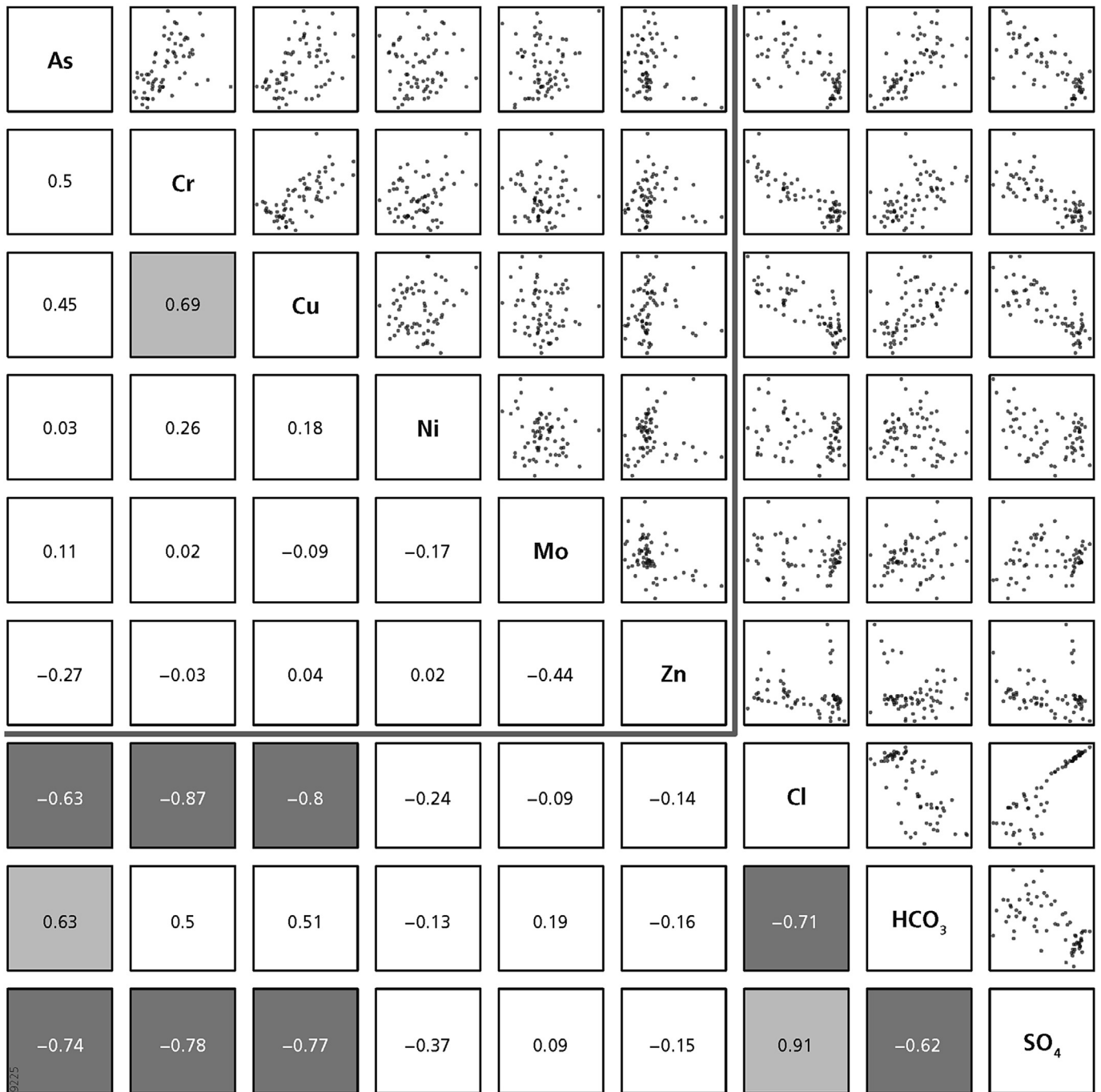


**Fig. 5.** Correlation matrix for the heavy metals and major ions Cl, SO<sub>4</sub> and alkalinity (as HCO<sub>3</sub>). The pale grey cells are positive correlations >0.6 and the dark grey cells show negative correlations of below -0.6.

amount of pyrite oxidation was calculated from the additional SO<sub>4</sub> relative from the mixing line. From section 3.2 we can infer that the maximum additional SO<sub>4</sub> was 215 ppm, which coincides with the oxidation of 1.1 mmol pyrite. We decided to calculate with three different amounts of pyrite oxidation: 0.5 mmol, 1 mmol and 1.5 mmol per L water as used in PHREEQC. The initial pyrite content of the sand profile was set at 1 g per kg sand, which is comparable to what is found.

In the first seawater scenario, we assume that both the carbonate-rich and the carbonate-poor sites are primarily affected by seawater. The calculations showed that the CaCO<sub>3</sub> will not diminish after the pyrite has oxidised, because seawater is

supersaturated for calcite and this will avoid CaCO<sub>3</sub> dissolution. This scenario is not affected when different pyrite contents are used. For the second rain water scenario a different situation occurs. The carbonate-rich site will oxidise pyrite (with a concentration of 0.5 mmol per L water) to a depth of 0.5 m in the sand profile in 89 years, but CaCO<sub>3</sub> will continue to dissolve, because rainwater is undersaturated in calcite. In total, 1768 years are needed to dissolve the CaCO<sub>3</sub> present in 0.5 m down the sand profile. The time required to dissolve the CaCO<sub>3</sub> to a depth of 0.5 m in the sand profile is 1759 years with a pyrite oxidation of 1 mmol per L water and 1754 years with a pyrite oxidation of 1.5 mmol per L water. For a carbonate-poor site with 1% CaCO<sub>3</sub> the total time

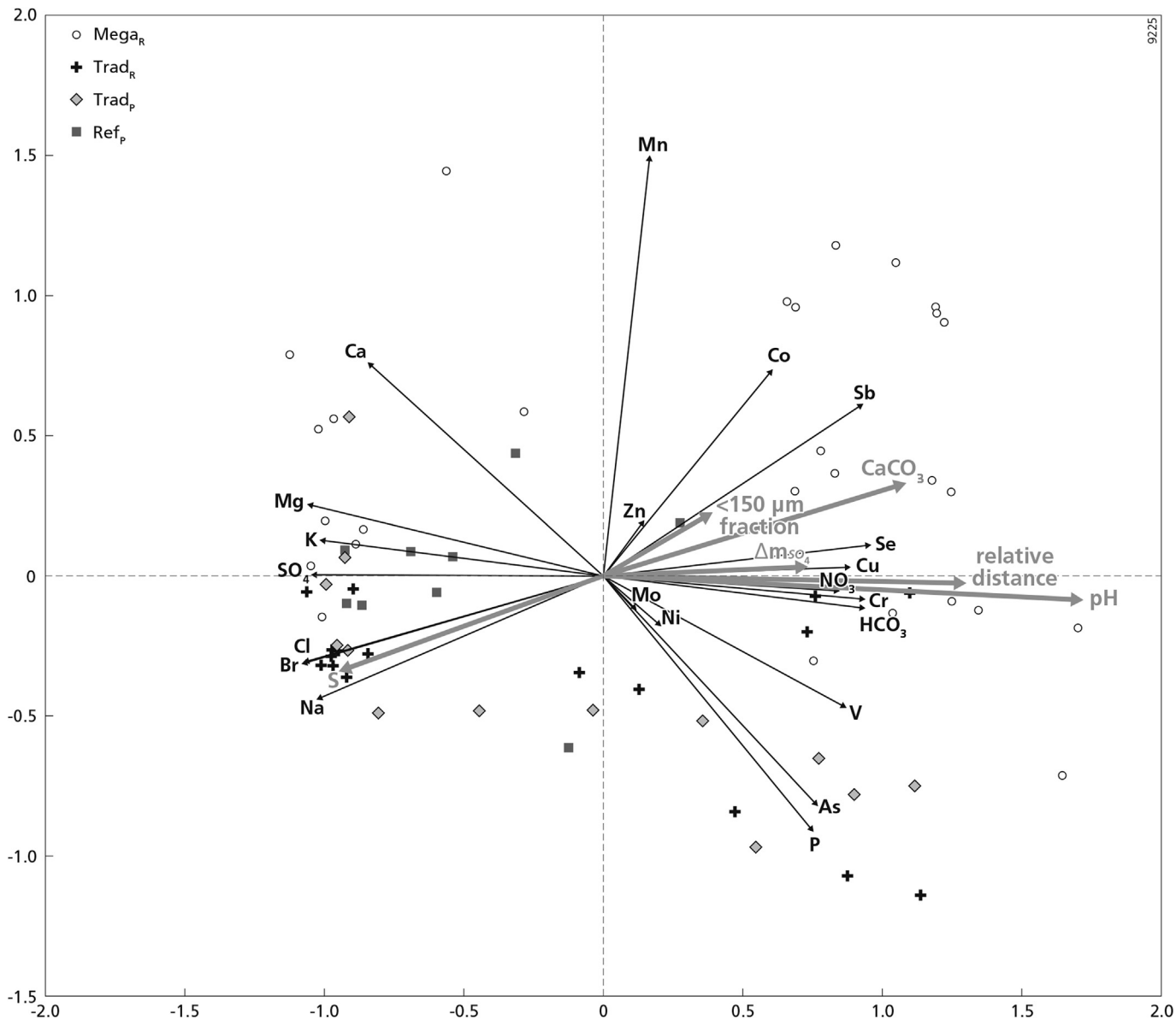


**Fig. 6.** An ordination diagram with two axes of a PCA of the pore water chemistry. The black arrows represent the different chemical elements and each symbol represents a different site. Six environmental variables shown by grey arrows are projected on top of the PCA.

required for decalcification are 361 years (scenario with a pyrite oxidation of 0.5 mmol per L water), 352 years (1 mmol per L water) and 348 years (1.5 mmol per L water).

For the rainwater scenarios, the dissolution of  $\text{CaCO}_3$  is 2.5–5 times higher when pyrite is present compared to the condition when pyrite is exhausted. The amount of time to oxidise 1 g per kg sand of pyrite present in a 0.5 m sand profile is 89 years (with a pyrite concentration of 0.5 mmol per L water), 45 years (with 1.0 mmol per L water) and 30 years (with 1.5 mmol per L water). Note that the expected lifespan of a mega beach nourishment is also 30 years (Stive et al., 2013). When the  $\text{CaCO}_3$  content becomes below 0.35%, the  $\text{CaCO}_3$  will dissolve within 30 years when a pyrite oxidation of 1.5 mmol per L water is present.

**4. Discussion**

Target Values for trace elements were regularly exceeded for pore water, especially at the beach nourishment sites, for Mo, Ni, Cr

and As, whereas the Intervention Values were exceeded sporadically. Pyrite oxidation contributes to the mobilisation of these elements, which happens mostly under fresh water conditions. At neutral pH, these trace elements become sorbed to Fe oxyhydroxides that are also produced during pyrite oxidation in an aerobic environment (Stumm and Morgan, 2012; Saulnier and Mucci, 2000). However, the presence of oxyanionic compounds of Mo, Cr and As may compete and as a result these trace elements remain mobilised (Langmuir, 1997; Paoletti, 2002). Additionally, dissolved As competes with other dissolved species as well, such as V,  $\text{PO}_4$  and Si, which may also inhibit adsorption (Stollenwerk, 2003; Johannesson and Tang, 2009). The relationship found between Cr and pH in the two carbonate-rich sites Mega<sub>R</sub> and Trad<sub>R</sub> may be related to the preference of Cr to adsorb to carbonatic phases; it can become remobilised when carbonate minerals go into solution (Shaheen and Rinklebe, 2015). The mobilisation of trace elements can be prevented by limiting the oxidation of material dredged from the sea floor. Long-term oxidation processes

can be limited by creating a nourishment with a thin unsaturated zone (like that at the reference site) or with no unsaturated zone at all (for example, a foreshore nourishment instead of a beach nourishment).

Trace element concentrations in the sediment did not exceed Intervention Values or Target Values at any of the sites and we found that the fine fraction of <150  $\mu\text{m}$  contained higher trace element contents than the total sediment, which was also observed by Sarkar et al. (2017). However, the fine fraction was generally small, with a limited amount of organic matter and associated low turnover and the nourishment sites had much stronger sorting than the reference location, probably because of dredging (Pit et al., 2017). We foresee that if the beach sand contains a significant fine fraction, the content of trace elements in pore water may be affected locally. With a concept like the Sand Engine, where the development of a spit is important and therefore aeolian activity should be encouraged, sorting processes may locally cause trace element content in the sediment to increase with time, to create a body of sand with relatively high trace element contents. The anomalous Ti content at Mega<sub>R</sub> compared to the Ti content at the other field sites may be related to geological differences, as Mega<sub>R</sub> contains material from two different geological layers (Pit et al., 2017).

The surface sediment samples were in general continuously unsaturated and redox potentials were found to be high as indicated by the absence of dissolved Fe. Therefore, chemical processes can mainly be focused on oxidation processes. However,  $\Delta m_{\text{SO}_4}$  and sedimentary S results indicate that reducing conditions of  $\text{SO}_4^{2-}$  occurs as well, especially at Ref<sub>p</sub> where Target Values for trace elements were less exceeded compared to the beach nourishment sites. Reducing conditions are only observed for saline pore water while trace elemental concentrations are low. This can be related to a short distance to the sea or a thin unsaturated zone, of which the latter is seen at Ref<sub>p</sub>. Therefore, with a high seawater content, the low concentrations of trace elements may be related to reducing conditions where freshly formed Fe-sulphides might immobilize trace elements (Frohne et al., 2011; Smith and Melville, 2004).

Besides pyrite oxidation, the influence of fresh water can be regarded as also encouraging the mobility of trace elements. Cationic trace elements such as Cr, Cu, Cd, Pb and Zn become more mobile under acid conditions (Salminen et al., 2005; Langmuir, 1997). We estimated that the sand profile at an initially carbonate-poor site with 0.35% can be decalcified to a depth of 0.5 m in 30 years when only affected by rainwater. This means that trace elements become more mobile when buffering capacity is limited and pH values decrease towards rainwater values (around pH = 5: Stolk, 2001). Higher concentrations of  $\text{CaCO}_3$  have been observed both in the Netherlands and elsewhere along coasts. For example, Pilkey et al. (1967) found  $\text{CaCO}_3$  concentrations of up to 45% along the southeastern coast of the United States. Also, in most natural environmental settings the buffering capacity will not drop, as most beaches are replenished by calcareous sand naturally or artificially within a short period of time. Further, in most environmental settings the sand is saturated with slightly alkaline seawater that has some buffering capacity (142 mg/L alkalinity (Hem, 1985)) rather than with rainwater. We conclude that nourishments with a  $\text{CaCO}_3$  content of below 0.4%, a lifespan of more than 30 years and are elevated well above mean sea level have a potential risk of metal mobilisation due to freshening of the sand by rainwater.

Compared to the rates reported by other dune studies on decalcification, our decalcification rate is relatively low. For example, Rozema et al. (1985) reported a decalcification rate of  $7.7 \cdot 10^{-3}$  per year, which would mean that the time required to become decalcified would be over 300 years for a carbonate-rich site (3.9%  $\text{CaCO}_3$ ) and 29 years for a carbonate-poor site (1%  $\text{CaCO}_3$ ).

Stuyfzand (1984) reported a decalcification constant 10 times lower, which would make the period required to decalcify longer and more comparable. However, these estimates are based on different processes like organic matter degradation at vegetated sites, which makes it difficult to compare our estimates with those reported in other studies.

## 5. Conclusions

Our study shows that elevated concentrations of trace elements are observed in the pore water of beach nourishments, but not in the sediment. The main driver is pyrite oxidation, especially where an unsaturated zone is present and rainwater influences are apparent. From the investigated sites, the mega beach nourishment shows the highest intensity of pyrite oxidation, because of its thickest unsaturated zone and predominantly fresh water conditions compared to the other sites. The reference site shows the lowest intensity of pyrite oxidation or even no oxidation, which is related to the low aeration possibilities of the beach sand because of a thin unsaturated zone. Target Values for trace elements are somewhat less exceeded at the mega beach nourishment compared to the traditional nourishments, which is most likely related to geological differences. To prevent trace metal mobility at a beach nourishment it is most important to maintain seawater influence in the shallow sand and to keep oxidation processes limited. This would indicate that a shoreface nourishment is to be preferred over a beach nourishment containing a thick unsaturated zone. Consequently, the difference between a carbonate-rich or a carbonate-poor site with presence of pyrite is of minor importance, because the influence of seawater will limit decalcification and large-scale oxidation processes and with that limit the risk that trace elements will be mobilised.

## Acknowledgements

This work was supported by NatureCoast, a project of Technology Foundation STW (12691), applied science division of the Netherlands Organisation for Scientific Research (NWO). The authors would like to thank Jerry van Dijk for the support and help with the Canoco 5 computer program and Isabel Trujillo Rocha for support on the field campaign. The authors' editor of a near-final draft of the paper was Joy Burrough. Comments from two reviewers are gratefully acknowledged as they have contributed to improve the manuscript.

## References

- Alshahri, F., 2017. Heavy metal contamination in sand and sediments near to disposal site of reject brine from desalination plant, Arabian Gulf: assessment of environmental pollution. *Environ. Sci. Pollut. Res.* 1–11. <http://dx.doi.org/10.1007/s11356-016-7961-x>.
- Appelo, C.A.J., Postma, D., 2005. *Geochemistry, Groundwater and Pollution*, second ed. A.A. Balkema Publishers, Leiden, The Netherlands, p. 683.
- Baak, J.A., 1936. Regional Petrology of the Southern North Sea. Ph.D-thesis. Leiden University, The Netherlands, p. 127.
- Benlahcen, K., Chaoui, A., Budzinski, H., Bellocq, J., Garrigues, P., 1997. Distribution and sources of polycyclic aromatic hydrocarbons in some Mediterranean coastal sediments. *Mar. Pollut. Bull.* 34, 298–305.
- Braak, C.J.F., Šmilauer, P., 2012. *CANOCO Reference Manual and User's Guide: Software for Ordination*. Microcomputer Power, Ithaca, New York, Version 5.0. .
- Brown, A.C., McLachlan, A., 2006. *The Ecology of Sandy Shores*, second ed. Academic Press, Burlington, p. 387.
- Bruce, J.R., 1928. Physical factors on the sandy beach. Part II. Chemical changes—carbon dioxide concentration and sulphides. *J. Mar. Biol. Assoc. U. K.* New Ser. 15, 553–565.
- Calmano, W., Hong, J., Förstner, U., 1993. Binding and mobilization of heavy metals in contaminated sediments affected by pH and redox potential. *Water Sci. Technol.* 28, 223–235.
- CBS, PBL, Wageningen UR, 2016. *Meteorologische Gegevens, 1990-2015*. CBS, Den Haag, Planbureau voor de Leefomgeving, Den Haag/Bilthoven en Wageningen

- UR, Wageningen.
- Chen, M., Ma, L.Q., 2001. Comparison of three aqua regia digestion methods for twenty Florida soils. *Soil Sci. Soc. Am. J.* 65, 491–499.
- De Vriend, H.J., Van Koningsveld, M., 2012. *Building with Nature: Thinking, Acting and Interacting Differently*. Ecoshape, Dordrecht, The Netherlands. <http://dx.doi.org/10.1080/02513625.2014.925714>.
- Egozcue, J.J., Pawłowsky-Glahn, V., Mateu-Figueras, G., Barceló-Vidal, C., 2003. Isometric logratio transformations for compositional data analysis. *Math. Geol.* 35, 279–300. <http://dx.doi.org/10.1023/A:1023818214614>.
- Eisma, D., 1968. Composition, origin and distribution of Dutch coastal sands between Hoek van Holland and the island of Vlieland. *Neth. J. Sea Res.* 4, 123–267.
- El-Kammar, A., Arafa, I., El-Sheltami, O., 2007. Mineral composition and environmental geochemistry of the beach sediments along the eastern side of the Gulf of Suez. *Egypt. J. Afr. Earth Sci.* 49, 103–114.
- Filzmoser, P., Hron, K., Reimann, C., 2009. Univariate statistical analysis of environmental (compositional) data: problems and possibilities. *Sci. Total Environ.* 407, 6100–6108. <http://dx.doi.org/10.1016/j.scitotenv.2009.08.008>.
- Fiselier, J., 2012. Projectnota/MER.Aanleg en zandwinning Zandmotor Delflandse kust (Sand Engine Delfland coast: project plan and assessment of the environmental impact report). DHV BV, Amersfoort, The Netherlands report no. C6158–01.001.
- Foteinis, S., Kallithrakas-Kontos, N.G., Synolakis, C., 2013. Heavy metal distribution in opportunistic beach nourishment: a case study in Greece. *Sci. World J.* 2013, 472149. <http://dx.doi.org/10.1155/2013/472149>.
- Frohne, T., Rinklebe, J., Diaz-Bone, R.A., Du Laing, G., 2011. Controlled variation of redox conditions in a floodplain soil: impact on metal mobilization and bi-methylation of arsenic and antimony. *Geoderma* 160, 414–424.
- Griffioen, J., Klaver, G., Westerhoff, W.E., 2016. The mineralogy of suspended matter, fresh and Cenozoic sediments in the fluvio-deltaic Rhine–Meuse–Scheldt–Ems area, the Netherlands: an overview and review. *Neth. J. Geosci.* 95, 23–107. <http://dx.doi.org/10.1017/njg.2015.32>.
- Hanson, H., Brampton, A., Capobianco, M., Dette, H., Hamm, L., Lastrup, C., Lechuga, A., Spanhoff, R., 2002. Beach nourishment projects, practices, and objectives—a European overview. *Coast. Eng.* 47, 81–111.
- Hem, J.D., 1985. *Study and Interpretation of the Chemical Characteristics of Natural Water*, third ed. Department of the Interior, US Geological Survey Water-Supply Paper 2254, p. 263.
- Houba, V., Van der Lee, J., Novozamsky, I., 1995. *Soil Analysis Procedures; Other Procedures (Soil and Plant Analysis, Part 5B)*. Dept Soil Sci Plant Nutr, Wageningen Agricultural University, p. 217.
- Ihaka, R., Gentleman, R., 1996. R: a language for data analysis and graphics. *J. Comput. Graph. Stat.* 5, 299–314.
- Johannesson, K.H., Tang, J., 2009. Conservative behavior of arsenic and other oxyanion-forming trace elements in an oxic groundwater flow system. *J. Hydrol.* 378, 13–28.
- Lafabrie, C., Pergent-Martini, C., Pergent, G., 2008. Metal contamination of *Posidonia oceanica* meadows along the Corsican coastline (Mediterranean). *Environ. Pollut.* 151, 262–268.
- Langmuir, D., 1997. *Aqueous Environmental Geochemistry*, first ed. Prentice Hall, Upper Saddle River, NJ, p. 600.
- Lijzen, J., Baars, A., Otte, P., Rikken, M., Swartjes, F., Verbruggen, E., Van Wezel, A., 2001. Technical Evaluation of the Intervention Values for Soil/sediment and Groundwater. Human and Ecotoxicological Risk Assessment and Derivation of Risk Limits for Soil, Aquatic Sediment and Groundwater. National Institute of Public Health and the Environment (RIVM), Bilthoven, The Netherlands report no. 711701 023.
- Moreira, F.T., Balthazar-Silva, D., Barbosa, L., Turra, A., 2016. Revealing accumulation zones of plastic pellets in sandy beaches. *Environ. Pollut.* 218, 313–321.
- Morton, A.C., 1984. Stability of detrital heavy tertiary sandstones from sea basin minerals in the north. *Clay Miner.* 19, 287–308.
- Paoletti, F., 2002. Behavior of Oxyanions Forming Heavy Metals in Municipal Solid Waste Incineration. Ph.D. Thesis. Univ. Stuttgart.
- Parkhurst, D.L., Appelo, C., 2013. Description of Input and Examples for PHREEQC Version 3—a Computer Program for Speciation, Batch-reaction, One-dimensional Transport, and Inverse Geochemical Calculations, p. 497. US geological survey techniques and methods, book 6.
- Pilkey, O.H., Morton, R.W., Luternauer, J., 1967. The carbonate fraction of beach and dune sands. *Sedimentology* 8, 311–327.
- Pit, I.R., Griffioen, J., Wassen, M.J., 2017. Environmental geochemistry of a mega beach nourishment in The Netherlands: monitoring freshening and oxidation processes. *Appl. Geochem.* 80, 72–89. <http://dx.doi.org/10.1016/j.apgeochem.2017.02.003>.
- Post, M.H., Blom, E., Chen, C., Bolle, L.J., Baptist, M.J., 2017. Habitat selection of juvenile sole (*Solea solea* L.): consequences for shoreface nourishment. *J. Sea Res.* 122, 19–24.
- Reimann, C., Filzmoser, P., Garrett, R., Dutter, R., 2011. *Statistical Data Analysis Explained: Applied Environmental Statistics with R*, vol. 2008. Wiley, Chichester, UK, p. 343.
- Rozema, J., Laan, P., Broekman, R., Ernst, W., Appelo, C., 1985. On the lime transition and decalcification in the coastal dunes of the province of North Holland and the island of Schiermonnikoog. *Acta Bot. Neerl.* 34, 393–411.
- Salbu, B., Steinnes, E., 1994. *Trace Elements in Natural Waters*. CRC Press, London, p. 314.
- Salminen, R., Batista, M., Bidovec, M., Demetriades, A., De Vivo, B., De Vos, W., Duris, M., Gilicis, A., Gregorauskiene, V., Halamić, J., 2005. *Geochemical Atlas of Europe, Part 1, Background Information, Methodology and Maps*. Geological survey of Finland.
- Sarkar, S.K., Mondal, P., Biswas, J.K., Kwon, E.E., Ok, Y.S., Rinklebe, J., 2017. Trace elements in surface sediments of the Hooghly (Ganges) estuary: distribution and contamination risk assessment. *Environ. Geochem. Health* 1–14.
- Saulnier, I., Mucci, A., 2000. Trace metal remobilization following the resuspension of estuarine sediments: Saguenay Fjord, Canada. *Appl. Geochem.* 15, 191–210.
- Seeberg-Elverfeldt, J., Schlüter, M., Feseker, T., Kölling, M., 2005. Rhizon sampling of pore waters near the sediment/water interface of aquatic systems. *Limnol. Oceanogr. Meth.* 3, 361–371.
- Shaheen, S.M., Rinklebe, J., 2015. Impact of emerging and low cost alternative amendments on the (im) mobilization and phytoavailability of Cd and Pb in a contaminated floodplain soil. *Ecol. Eng.* 74, 319–326.
- Shaheen, S.M., Rinklebe, J., 2017. Sugar beet factory lime affects the mobilization of Cd, Co, Cr, Cu, Mo, Ni, Pb, and Zn under dynamic redox conditions in a contaminated floodplain soil. *J. Environ. Manage.* 186, 253–260.
- Smith, J., Melville, M.D., 2004. Iron monosulfide formation and oxidation in drain-bottom sediments of an acid sulfate soil environment. *Appl. Geochem.* 19, 1837–1853.
- Speybroeck, J., Bonte, D., Courtens, W., Gheskiere, T., Grootaert, P., Maelfait, J., Mathys, M., Provoost, S., Sabbe, K., Stienen, E.W., 2006. Beach nourishment: an ecologically sound coastal defence alternative? A review. *Aquat. Conserv. Mar. Freshwat. Ecosyst.* 16, 419–435.
- Stive, M.J., de Schipper, M.A., Luijendijk, A.P., Aarninkhof, S.G., van Gelder-Maas, C., van Thiel de Vries, Jaap S.M., de Vries, S., Henriquez, M., Marx, S., Ranasinghe, R., 2013. A new alternative to saving our beaches from sea-level rise: the sand engine. *J. Coast. Res.* 29, 1001–1008. <http://dx.doi.org/10.2112/JCOASTRES-D-13-00070.1>.
- Stolk, A.P., 2001. Landelijk meetnet regenwatersamenstelling, meetresultaten 2000 (in Dutch). National Institute of Public Health and the Environment (RIVM), Bilthoven, The Netherlands. report no. 723101 057.
- Stollenwerk, K.G., 2003. Geochemical processes controlling transport of arsenic in groundwater: a review of adsorption. In: *Arsenic in Ground Water*. Kluwer, Academic Publishers, Boston, pp. 67–100.
- Stumm, W., Morgan, J.J., 2012. *Aquatic Chemistry: Chemical Equilibria and Rates in Natural Waters*, third ed. John Wiley & Sons, New York, p. 1040.
- Stuyfzand, P.J., 1984. Effecten van vegetatie en luchtverontreiniging op de grondwaterkwaliteit in kalkrijke duinen bij Castricum: lysimeterwaarnemingen, pp. 152–159 (in Dutch). H2O (17) 8.
- Stuyfzand, P.J., Arens, S.M., Oost, A.P., Baggelaar, P.K., Adviesbureau, I.S., 2012. *Geochemische effecten van zandsuppleties in Nederland (in Dutch)*. Bosschap, The Hague, The Netherlands. report no. 2012/OBN167-DK.
- Swartjes, F.A., Rutgers, M., Lijzen, J.P.A., Janssen, P.J.C.M., Otte, P.F., Wintersen, A., Brand, E., Posthuma, L., 2012. State of the art of contaminated site management in The Netherlands: policy framework and risk assessment tools. *Sci. Total Environ.* 427–428, 1–10. <http://dx.doi.org/10.1016/j.scitotenv.2012.02.078>.
- Van Bruggen, M., Swartjes, F., Janssen, P., Pit, I., Griffioen, J., Spijker, J., 2014. Beoordeling gezondheidsrisico's van arseen op de Zandmotor (in Dutch). National Institute of Public Health and the Environment (RIVM), Bilthoven, The Netherlands. report no. 2014–0063.
- Van Dalftsen, J.A., Essink, K., 2001. Benthic community response to sand dredging and shoreface nourishment in Dutch coastal waters. *Mar. Biodivers.* 31, 329–332.
- Vetrimurugan, E., Shruti, V., Jonathan, M., Roy, P.D., Kunene, N., Villegas, L.E.C., 2017. Metal concentration in the tourist beaches of South Durban: an industrial hub of South Africa. *Mar. Pollut. Bull.* 117 (1), 538–546. <http://dx.doi.org/10.1016/j.marpolbul.2017.02.036>.
- VROM, 2009. *Circulaire Bodemsanering 2009*. Staatscourant 7 april 2009, nr 67.
- Wilcoxon, F., 1945. Individual comparisons by ranking methods. *Biom. Bull.* 1, 80–83.